Modulated Imaging: A novel method for quantifying tissue chromophores in evolving cerebral ischemia

David Abookasis,[a] Marlon S. Mathews,[a,b] Christopher Lay,[c] Ron D. Frostig,[c] and Bruce J. Tromberg [a,d]

[a] Beckman Laser Institute and Medical Clinic, University of California, Irvine, CA 92612.
[b] Department of Neurological Surgery, University of California, Irvine, Medical Center, Orange, CA 92868.
[c] Department of Neurobiology and Behavior, University of California, Irvine, CA 92697.
[d] Department of Biomedical Engineering, the Henry Samueli School of Engineering, University of California, Irvine, CA 92697.

ABSTRACT

The authors report the results of utilizing spatially-modulated near infrared light using Modulated Imaging (MI) technology in imaging cerebral ischemia. MI images of the left parietal somatosensory cortex were obtained post-occlusion and up to three hours following middle cerebral artery occlusion. Tissue chromophore maps were obtained to demonstrate spatiotemporal changes in the distribution of oxy, deoxy, total hemoglobin, and oxygen saturation. MI recorded a decrease in oxyhemoglobin concentration and tissue oxygen saturation and increase in tissue deoxyhemoglobin concentration following occlusion. Optical intrinsic signal was used to detect functional activation of the somatosensory barrel cortex to whisker stimulation. This activation was completely lost following occlusion. Imaging findings in a transient ischemic attack using photothrombosis is also demonstrated.

Keywords: Modulated Imaging, Stroke, Ischemia, Brain Attack, MCA stroke, TIA.

1. INTRODUCTION

Optical methods in medicine and particularly for brain imaging provide an alternative imaging modality with great potential to clinical diagnostics.[1,2] One of the major growing areas of interest is in the field of neuroimaging and the ability to detect changes in the cerebral hemoglobin oxygenation during brain ischemia. Brain ischemia results from the sudden reduction of blood flow to brain tissue below tissue sustainable levels leading to neuronal dysfunction.[3] During ischemia there are changes in the concentrations of oxyhemoglobin, deoxyhemoglobin, and water in brain tissue.[4-6] These molecules absorb specific wavelengths of light which alters the optical properties of brain tissue.[7,8] Existing imaging techniques such as magnetic resonance imaging (MRI) do not quantify tissue concentrations of oxyhemoglobin, deoxyhemoglobin, and water; rather they detect relative changes from a referenced baseline.[9] In this study we propose a significantly different platform (depicted in Fig. 1) to detect these alterations and quantitatively map changes in oxyhemoglobin, deoxyhemoglobin and oxygen saturation, during acute ischemic injury of the brain using a new approach based on the spatial modulation of white light.[10] In order to demonstrate the ability of our technique to quantify hemodynamic activity in the brain during the injury, we chose to focus on two different types of acute injury in the rat brain as follows: large strokes, and small strokes. Strokes (cerebrovascular accident or CVA), results from vascular disease affecting the arteries supplying blood to the brain and occurs when one of these vessels bursts or is clogged.[11] The most commonly involved artery is the Middle Cerebral Artery (MCA).[12] Transient ischemic attack (TIA) is a reversible ischemic injury to the brain that occurs when a blood clot temporarily clogs an artery and blood supply to part of the brain is compromised.[13] The symptoms, which are the same as stroke symptoms, occur

Medical Imaging 2007: Physiology, Function, and Structure from Medical Images, edited by Armando Manduca, Xiaoping P. Hu, Proc. of SPIE Vol. 6511, 65110A, (2007) · 1605-7422/07/$18 · doi: 10.1117/12.713470

rapidly and last for a few minutes to a few hours. Clinically, TIA is associated with cognitive deterioration and vascular dementia, and are major risk factors for large strokes. We used a photothrombosis model using intravascular Rose Bengal, which when excited by green light releases singlet oxygen which damages capillary endothelium and produces reversible thrombosis. This is an established model for inducing reversible ischemia previously demonstrated by Schaffer *et. al*.[14]

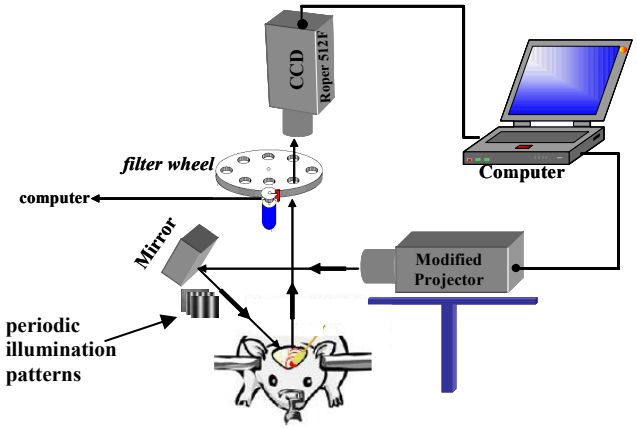

Figure. 1: Layout of the optical projection system.

2. MATERIALS AND METHODS

2.1 Imaging Instrument

A schematic diagram of our experimental setup is shown in Fig. 1. Periodic illumination patterns of two spatial frequencies with a 120º phase shifting between three adjacent patterns are projected onto the brain from a conventional projector based digital micromirror device (DMD). The diffusely reflected light (the deformed fringe pattern) passes through 10nm-wide bandpass filters (Andover Corp.) and is then recorded by a CCD camera (Roper Scientific, 512F), which features an 512×512 imaging array covering the spectral range between 400nm and 1000nm. Five bandpass filters (680, 720, 760, 800 and 980nm, at times we used 880nm instead of 980nm) are placed on a five position automatic filter wheel (Spectral Product, AB302). The demodulation of the reflectance spatially-modulated light characterizes the modulation transfer function of the diffuse reflectance of the brain and contains structural and functional information of the brain. To determine quantitatively the absorption (μ_a) and reduced scattering (μ_s') coefficients, and hence also the chromophores parameters, we used the diffusion approximation to the radiative transport theory with Monte Carlo simulation[15] to relate the measured reflected light intensity to the optical coefficients through MATLAB technology (Ver 7.04). The entire system is controlled by a personal computer through the LabView platform (Ver 7).

2.2 Surgical Procedure

Adult male Sprague-Dawley rats were anesthetized and their heads were fixed on a stereotactic apparatus in order to create an imaging window. A midline skin incision was made and 5x5mm square area overlying the left somatosensory cortex was outlined. The skull over this area was thinned with a dental drill (to about 100μm) until the middle cerebral artery and superior cerebral veins were visible. A thin film of agarose was made over the thinned area of skull. The agarose film was covered with a coverglass and the entire set up served as an imaging window. The agarose is filled in

the cranial window to prevent the skull from drying and to increase its transparency to the light. Specific procedures in each experimental group are discussed under the following section.

2.2.1 Middle Cerebral Artery Occlusion (MCAo)

In addition to the following surgical procedures outlined above, a craniotomy was performed on the left side of the brain as the imaging window to expose the MCA. The MCA was surgically cauterized using monopolar cautery to produce MCA occlusion.

2.2.2 Transient ischemic attack or TIA

Adult male Sprague-Dawley rats underwent the same surgical procedure to create an optical imaging window as outlined in the Section 2.2.1. 3% (wt/vol) Rose Bengal dye (Sigma, St. Louis, MO) in isotonic saline was injected through the tail vein, following which, four branches of the MCA supplying the barrel cortex were identified, using a CCD camera and a green illumination. To optically excite Rose Bengal and produce thrombosis[14] a continuous wave 532nm laser beam (EO, NT53-768) with 1mw average power (after attenuation) was directed into the aforementioned surface branches of the MCA with illumination of 10 minutes at each location.

2.3 Imaging Procedure

Imaging was performed through the surgically created imaging window on the anesthetized rats held in a stereotactic frame. The reflected image of the ROI of the cortex was acquired on a CCD camera while projecting spatially modulated light onto the ROI. The modulated images were obtained from ROI selected by the investigators, and processed to obtain quantitative oxy and deoxy hemoglobin maps. These maps were generated every minute to study the changes in cortical perfusion with time following experimental manipulation. Imaging was started before induction of experimental ischemia to establish baseline concentrations of oxyhemoglobin, deoxyhemoglobin, and hemoglobin oxygen saturation and repeated during and after experimental intervention. The animal remained anesthetized during the entire imaging procedure.

Animal housing, care, and experimental protocols were carried out in conformity with the guidelines of the United States National Institutes of Health. The laboratory animal protocol for this work was approved by the Institutional Animal Care and Use Committee (IACUC) at the University of California, Irvine and by the U. S. Department of Defense (DOD).

3. RESULTS AND DISCUSSION

3.1 MCAo Results

The demonstration of the mean optical properties (μ_a and μ_s' in units of mm^{-1}) spectra and mapping recovered at 680nm after the occlusion at the end of the experimental session is shown in Fig. 2. In Fig 2(*a*) we show the averaged optical properties versus wavelength over the ROI (5×5 mm) retrieved from measurements using the solution of the steady state diffusion equation for a semi-infinite medium for spatial illumination source. The fitting values of the absorption and the scattering (blue curve) agreed well with their actual values (red circle) and the error in μ_a and μ_s' at all wavelengths were 3% and 6% respectively. These errors are mainly due to errors occurring in the calibration procedures (not detailed in this paper). It is well known through Mie theory that the reduced scattering coefficient in the NIR is wavelength dependence and can be approximate by: $\mu_s' = A\lambda^{-B}$, where A is a constant, λ is the wavelength (in nm), and B is the scatter power.[16-18] In this experiment we found that A=24 and B=0.55.

In Fig. 2(*b*) we show the mapping of these properties over the ROI at 680nm. Seen in the upper left of Fig. 2(*b*) is strong absorption at this wavelength in a vein from deoxy-hemoglobin in venous blood. Below each map is histogram distribution of the corresponding quantitative maps, highlighting the spatial variation in recovered optical properties. To validate the accuracy of these results we used the Monte Carlo computation of the inverse problem. The resulting optical properties were found to agree well between the two methods. By mapping the absorption coefficient at each wavelength, we can perform quantitative spectroscopy of tissue. Knowledge of the extinction coefficients of the tissue chromophores allows us to fit these spectra to a linear Beer-Lambert absorption model.[19] Consequently, we arrive at the quantitative concentrations of each chromophore after the occlusion, shown in Fig. 3. Notice the low and high concentration of oxy and deoxy-hemoglobin, respectively, over the vein regions. This effect can be emphasized by calculating the tissue-level oxygen saturation (S_tO_2 = 100*(HbO_2/[HbO_2+Hbr])), highlighting the effect of tissue oxygen extraction. The summation of HbO_2 and Hbr yields the total hemoglobin concentration (THC). Note that this quantitative, micromolar concentration is a direct, absolute measure of blood volume. The average results obtained from these maps yield concentrations for HbO_2, Hbr, THC and StO_2 of 35μM, 54μM, 89μM and 40%, respectively.

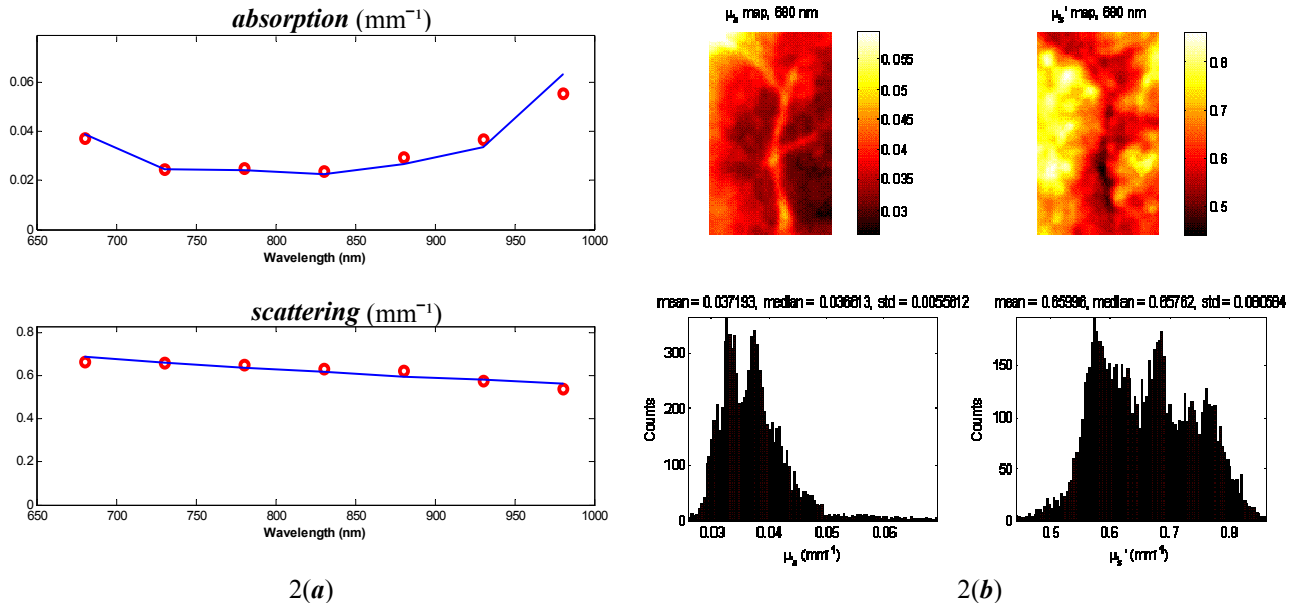

2(*a*) 2(*b*)

Figure. 2: (***a***) Average absorption and reduced scattering (in units of mm^{-1}) spectra over entire ROI. The blue line represents the fitting of the theory to the experiment (red circle). (***b***) Top: Quantitative Absorption (left) and scattering (right) maps at 680nm over the ROI. Bottom: histograms corresponding to above maps showing statistical distribution of recovered map values.

A comparison of the changes in the Hbr and S_tO_2 maps pre and post the occlusion are shown in Figure 4. Averaging over each of these maps we found a 15% increase in deoxy-hemoglobin concentration and a 20% decrease in hemoglobin oxygen saturation from a baseline measurement respectively following MCA occlusion. These changes reflect the pathophysiologic state of the brain and the ability of spatially modulated light to quantify changes in chromophore concentration with time.

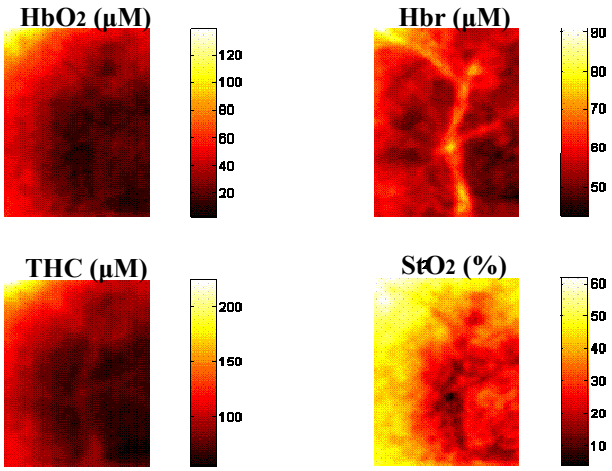

Figure. 3: Quantitative hemodynamic mapping of the cortex after the occlusion at the end of the experimental session. Higher concentration values correspond to brighter pixel scale values represents by the scale bar in the right of each panel.

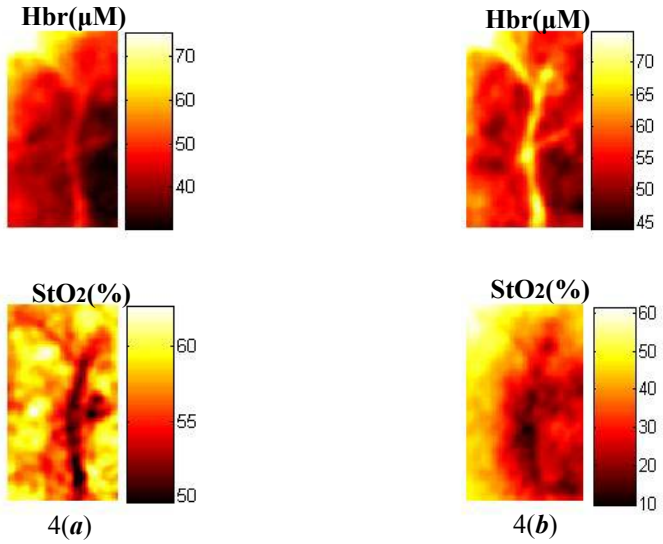

4(***a***) 4(***b***)

Figure. 4: Deoxyhemoglobin and oxygen saturation maps pre(***a***) (baseline) and post (***b***) MCAo.

Optical intrinsic signal (OIS)[20] is a functional neuroimaging technique that can map a large region of the cortex with spatial resolution of ~50μ. OIS images relative changes in the local concentration of deoxyhemoglobin as a surrogate marker for neuronal activity. Figure 5(*a)* shows OIS in the first 1.5s (500 ms in each frame) evoked in the barrel cortex

to whisker stimulation of an intact (control) rat under general anesthesia. Following MCAo, OIS signals were lost to whisker stimulation in the rat barrel cortex as shown in Fig. 5*(b)*.

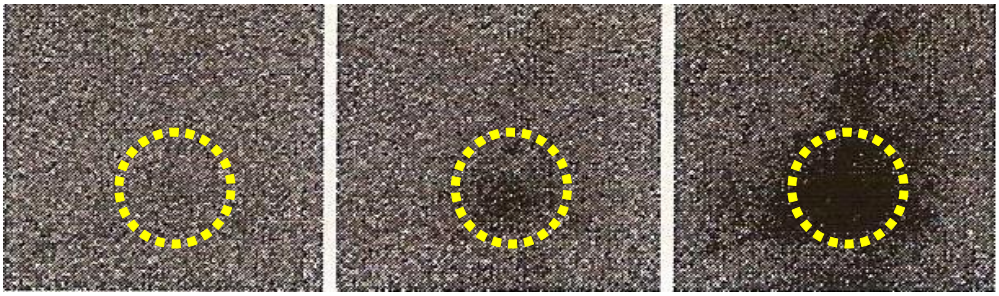

5(***a***)

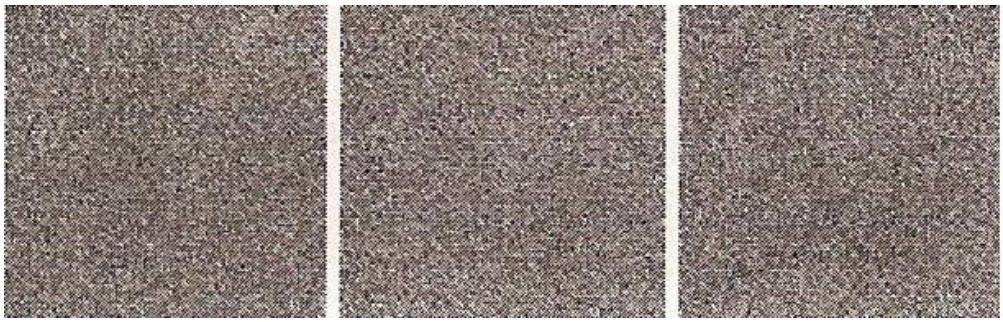

5(***b***)

Figure. 5: Images show the relative reflectance after stimulus onset. ***(a)*** represent the pre occlusion signal images while ***(b)*** represent the post MCAo signal images. In comparison to the data shown in ***(a)***, no functional activity is detected in ***(b)***.

3.2 TIA Results

Thrombosis was introduced by optical excitation of Rose Bengal using green laser in the temporary stroke experiment. This is an established model for inducing reversible ischemia already demonstrated by Schaffer *et. al*.[9] To assist with visualizing the blood flow while inducing the stroke, we inject through the tail-vein a fluorescent contrast agent Fluorescein-conjugated Dextran (FITC) prior to the Rose Bengal injection. Since excitation of FITC by blue light causes a fluorescent emission in the green region, we used a blue LED source and green filter in the front of the camera to visualize and to confirm the production of thrombosis. Clots are characterized by non-fluorescent region of densely packed cells. Under the CCD camera with green LED illumination, candidate vessels for photochemical blockage were identified and their position noted. Image of the cortex sixty-three minutes after 10 min of 532nm laser illumination for phototrombosis were acquired and analyzed. An example of the changes in the optical properties and chromophore concentration over time and space after the arteries occlusion are depicted in Fig. 6. Photothrombosis was followed by an increase in tissue deoxy-Hb concentration from the baseline and a decrease in Oxy-Hb and changes in optical properties. Between 84-86min after photothrombosis we observed changes in both optical properties and chromophore concentration which plateaued for the remainder of the imaging session. This reversal was probably from spontaneous thrombolysis occurring in one or more of the four illuminated arteries. Further study is on the way to validate this observation.

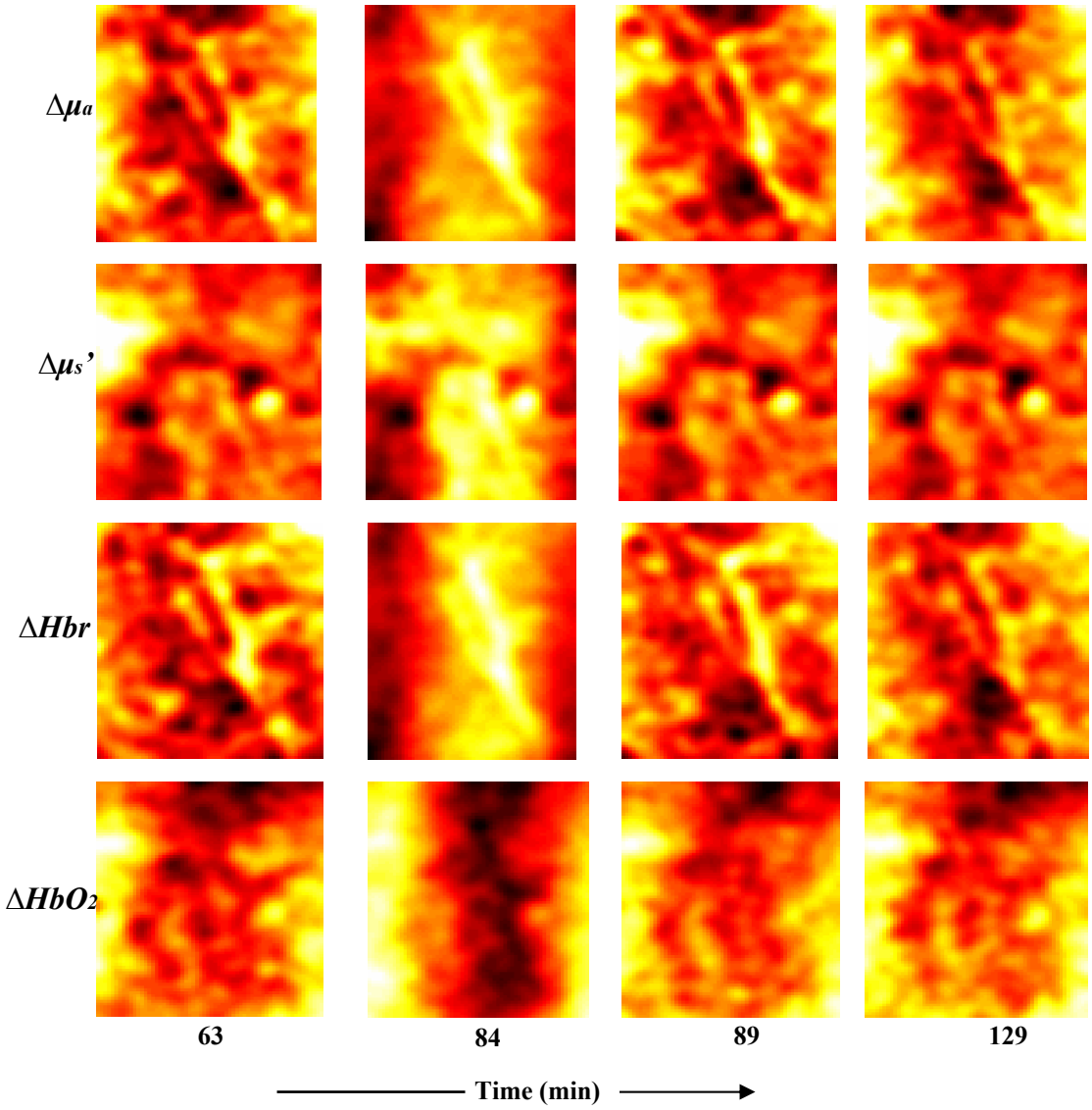

Figure. 6: Spatiotemporal distribution maps changes of absorption, reduced scattering, deoxyhemoglobin and oxyhemoglobin at 63, 84, 89 and 129 minute timepoints after Rose Bengal injection and 532nm illumination.

4. CONCLUSION

In this paper, we have demonstrated a powerful technique that provides quantitative information on the spatiotemporal distribution of physiologic parameters during brain ischemia in the rats using structured light. Two different pilot studies to map ischemic injury in the rodent barrel cortex namely MCAo, and TIA were demonstrated. Although, a number of studies relating to the application of optical modalities in the brain have been presented during the last thirty years to the best of our knowledge, this is the first work describing the use of spatial modulation of light for mapping

acute changes in tissue concentrations of physiologic chromophores over time in response to ischemia and separates absorption from scattering. We believe that spatial modulation of light can be useful for quantitative chromophore mapping of the brain and has a great potential for monitoring brain diseases which is of great significance to the neuroscience community. The results presented in this work are preliminary, and more work is currently in progress.

ACKNOWLEDGMENTS

This study has been funded by Laser Microbeam and Medical Program (LAMMP), a NIH Biomedical Technology Resource, grant #P41-RR01192, the U.S. Air Force Office of Scientific Research (AFOSR), Medical Free-Electron Laser (MFEL) Program (F49620-00-2-0371 and FA9550-04-1-0101) and the Beckman Foundation. Mr. Abookasis gratefully acknowledges the support of the Rothschild Foundation (Yad Hanadiv) Post-doc Research Fellowship Program, Israel. The authors would also like to thank Zhou *et.al.*[21] for permission to use the image of the rat shown in Fig. 1. E-mail may be addressed to dabookas@uci.edu

REFERENCES

1. R. D. Frostig, *In Vivo Optical Imaging of Brain Function*, (CRC Press, 2001).
2. G. Boas, "Noninvasive imaging of the brain," Optics News. **15**, pp. 52-55 (2004).
3. U. Dirnagl, C. Iadecola, and M.A. Moskowitz, "Pathobiology of ischaemic stroke : an integrated view," Trends Neurosci. **22**, pp. 391-397 (1999).
4. J. S. Wyatt, M. Cope, D. T. Delpy, S. Wray, and E. O.R. Reynolds, "Quantification of cerebral oxygenation and homodynamic in sick newborn infants by near infrared spectrophotometry," Lancet. **2**, pp. 1063-1066 (1986).
5. J. P. Culver, T. Durduran, T. Furuya, C. Cheung, J. H. Greenberg, and A. G. Yodh, "Diffuse optical tomography of cerebral blood flow, oxygenation, and metabolism in rat during focal ischemia," J. Cereb. Blood Flow Metab. **23**, pp. 911-924 (2003).
6. C. S. Robertson, S. P. Gopinath, and B. Chance, "Use of near-infrared spectroscopy to identify traumatic intracranial hemotomas," J. Biomed. Optics. **2**, pp. 31-41 (1997).
7. A. Villringer, and B. Chance, "Noninvasive optical spectroscopy and imaging of human brain function," Trends Neurosci. **20**, pp. 435-442 (1997).
8. F. Bevilacqua, D. Piguet, P. Marquet, J. D. Gross, B. J. Tromberg, and C. Depeursinge, "In Vivo local determination of tissue optical properties: applications to human brain," Appl. Opt. **38**, pp. 4939-4950 (1999).
9. J. G. Webster, *Minimally Invasive Medical Technology*, (IoP, Bristol and Philadelphia, 2001), Chap. 4, pp. 46-58.
10. D. J. Cuccia, F. Bevilacqua, A. J. Durkin, and B. J. Tromberg, "Modulated imaging: quantitative analysis and tomography of turbid media in the spatial-frequency domain," Opt. Lett. **30**, pp. 1354-1356 (2005).
11. L. R. Caplan, *Stroke*, (AAN Press, 2006).
12. S. T. Chen, C. Y. Hsu, E. L. Hogan, H. Maricq, and J. D. Balentine," A model of focal ischemic stroke in the rat: reproducible extensive cortical infarction," Stroke. **17**, pp. 738-743 (1986).
13. S. Chaturvedi, and S. R. Levine, *Transient Ischemic Attack*, (Blackwell Publishing, 2004).
14. C. B. Schaffer, B. Friedman, N. Nishimura, L. F. Schroeder, P. S. Tsai, F. F. Ebner, P. D. Lyden, and D. Kleinfeld, "Two-Photon imaging of cortical surface microvessels reveals a robust redistribution in blood flow after vascular occlusion," PLoS Biol. **4**, pp. 258-270 (2006).
15. F. Bevilacqua and C. Depeursinge, "Monte Carlo study of diffuse reflectance at source-detector separations close to one transport mean free path," J. Opt. Soc. Am. A. **16**, pp. 2935-2945 (1999).

16. R. Graaff, J. G. Aarnoose, J. R. Zijp, P. M. A. Sloot, F. F. M. de Mul, J. Greve, and M. H. Koelink, "Reduced light-scattering properties for mixtures of spherical particles: a simple approximation derived from Mie calculations," Appl. Opt. **31**, pp. 1370-1376 (1992).
17. J. R. Mourant , T. Fuselier , J. Boyer, T. Johnson, and I. J. Bigio, "Predictions and measurements of scattering and absorption over broad wavelength ranges in tissue phantoms," Appl. Opt. **36**, pp. 949-957 (1997).
18. J. M. Schmitt and G. Kumar, "Optical scattering properties of soft tissue: a discrete particle model," Appl. Opt. **37**, pp. 2788- 2797 (1998).
19. D. T. Delpy, M. Cope, P. van der Zee, S. Arridge, S. Wray, and J. Wyatt, "Estimation of optical pathlength through tissue from direct time of flight measurement," Phys. Med. Biol. **33**, pp. 1433-1442 (1988).
20. A. Grinvald, E. Lieke, R. D. Frostig, C. D. Gilbert, and T. N. Wiesel, "Functional architecture of cortex revealed by optical imaging of intrinsic signals," Nature. **324**, pp. 361-364 (1986).
21. C. Zhou, G. Yu, D. Furuya, J. Greenberg, A. Yodh, and T. Durduran, "Diffuse optical correlation tomography of cerebral blood flow during cortical spreading depression in rat brain," Opt. Exp. **14**, pp. 1125-1144 (2006).